Tectonophysics 546-547 (2012) 1–9

Contents lists available at SciVerse ScienceDirect

Tectonophysics

journal homepage: www.elsevier.com/locate/tecto

Evolution of the temporal multifractal scaling properties of the Chiayi earthquake ($M_L = 6.4$), Taiwan

Yi-Jiun Tang [a], Young-Fo Chang [a,*], Tai-Sheng Liou [a], Chien-Chih Chen [b], Yih-Min Wu [c]

[a] Institute of Seismology, National Chung Cheng University, Chiayi, Taiwan
[b] Institute of Geophysics, National Central University, Taoyuan, Taiwan
[c] Department of Geosciences, National Taiwan University, Taipei, Taiwan

ARTICLE INFO

Article history:
Received 8 June 2010
Received in revised form 22 March 2012
Accepted 4 April 2012
Available online 20 April 2012

Keywords:
Multifractal
Seismicity
Seismogenic regimes
Precursor of a large earthquake

ABSTRACT

Variations in the fractal dimension of earthquakes have been suggested to be a precursor of a large earthquake. However, the physical characteristics and seismicity are always different along a large fault system, and it is difficult to segment a large fault for further investigating. Therefore, the fractal dimension of earthquakes on a given fault only reflects the average seismic characteristics of the area and may be unrelated to precursory activity. In this paper, the evolution of the temporal generalized fractal dimension (D_q) of a seismic cluster within a small fault system associated with the Chiayi earthquake ($M_L = 6.4$), Taiwan, is investigated. The earthquakes of this sequence are confined in small source volume and reflect the behavior of the local fault system.

Our results show that the D_q curve of the background stage is smooth with a low multifractal degree (0.36) and the seismicity is nearly monofractal in the Chiayi region. During the foreshock stage, the seismicity becomes active such that not only the D_q curve exhibits greater variability especially for the steep slope of D_q curve at $q = 0$ but also the temporal fractal dimension changes from nearly monofractal to multifractal. In the aftershock stage, the fluctuation of D_q is large and the multifractal degree is up to 1.0. The temporal multifractal property becomes more pronounced as well. Finally, when the seismicity returns to the background stage, the D_q curve becomes smooth and nearly monofractal again. Therefore, the fluctuations in the D_q spectrum of an earthquake cluster associated with a large earthquake not only give a clear picture of the temporal alterations in the seismogenic regimes but also illustrate their variability through time for a large earthquake. In addition, the variation of the slope of D_q curve at $q = 0$ in the foreshocks may be used as a precursor of a large earthquake.

1. Introduction

Mandelbrot (1967) proposed a new concept of the geometric dimension, the fractal dimension, to estimate the complexity of the geometry of natural phenomenon. This concept has been used to estimate the fractal dimensions of fault traces and the distributions of epicenters and hypocenters (Aviles et al., 1987; Guo and Ogata, 1995; Henderson et al., 1999; Okubo and Aki, 1987; Öncel et al., 1996). Multifractal is one kind of fractal dimension defined as a union of several monofractals (Mandelbrot, 1989). Nowadays, multifractal has become one of the scaling laws to characterize the dynamic system, for example, the seismogenic regime.

Spatial multifractal properties of earthquakes have been used to analyze the spatial distributions of earthquakes (Hirata and Imoto, 1991; Mittag, 2003; Nakaya and Hashimoto, 2002). In terms of the temporal fractal analysis of earthquakes, the fractal dimension of the temporal distribution of earthquakes represents the clustering strength (Papadopoulos and Dedousis, 1992). The temporal multifractal variation of seismicity implies the variation of the degree of clustering over time (Godano and Caruso, 1995). In addition, the temporal multifractal variations of earthquake swarms mean the changes in the seismogenic regime (Mittag, 2003).

Hirabayashi et al. (1992) analyzed the temporal multifractal of seismicity in California, Japan and Greece. They concluded that when a large earthquake occurs, the fluctuations of temporal multifractal properties of earthquakes change and become more violent. They defined two types of multifractal spectra — steep type and smooth type. According to the spatial fractal analysis (Godano et al., 1999; Rossi, 1990), the epicenters of earthquakes will cluster before and after a large main shock. However, the physical characteristics and seismicity are always complex within a large fault system, so the fractal geometries of the seismicities along the San Andreas fault (Okubo and Aki, 1987), Sumatra fault (Sukmono, 2001) and Chelungpu (Chi-Chi earthquake) fault (Chang et al., 2007) are different. It is difficult to segment a large fault for further investigation. Hence, the multifractal variations of seismicity only reflect the average effect of seismicity within a large fault system.

* Corresponding author. Tel.: +886 5 272 0411x66208; fax: +886 5 272 0807.
E-mail address: seichyo@ccu.edu.tw (Y.-F. Chang).

0040-1951/$ – see front matter © 2012 Elsevier B.V. All rights reserved.
doi:10.1016/j.tecto.2012.04.006

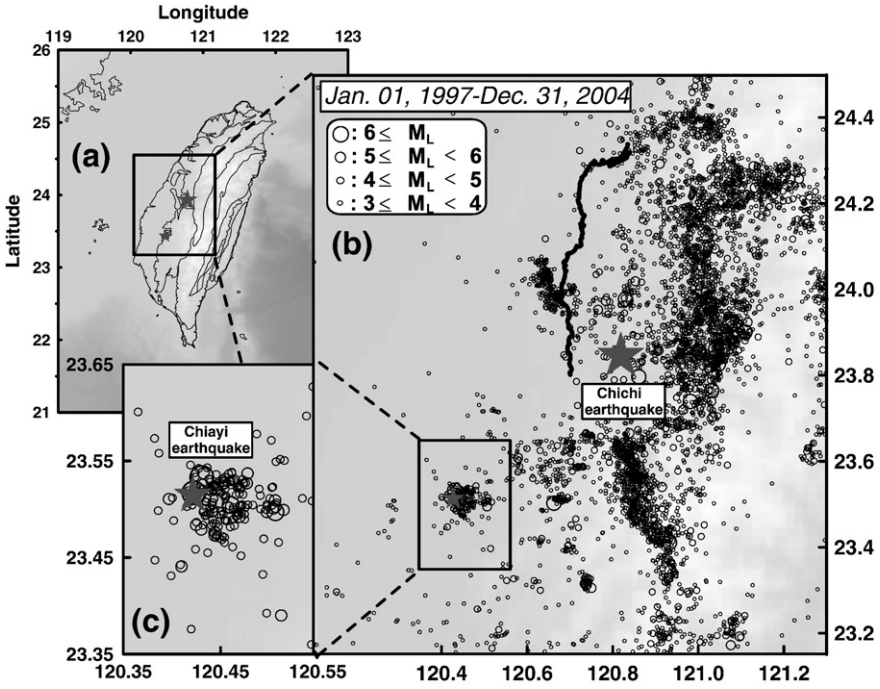

Fig. 1. Seismicity in Central Taiwan and the location of the study area. (a) Taiwan is a collision zone of the Asian-Europe plate and the Philippine plate. (b) Distributions of epicenters in Central Taiwan from January 1, 1997 to December 31, 2004. The big star sign indicates the location of the Chichi earthquake, and the small star sign indicates the location of the Chiayi earthquake. (c) The study area from 120.35°E to 120.55°E and from 23.35°N to 23.65°N (0.2°×0.3°). The star sign indicates the location of the Chiayi earthquake.

In this study, we analyze the multifractal variation of seismicity within a small fault system where the earthquakes are confined in small source volume and reflect the behavior of the fault system (Wen et al., 2008) to test whether the temporal multifractal fluctuation of the seismicity can show the evolvement of a large earthquake.

2. Tectonic setting and data

On October 22, 1999, an earthquake of magnitude 6.4 occurred in Chiayi, Taiwan. Hereafter, this earthquake is referred to as the Chiayi earthquake. The earthquake resulted in 5 deaths and 25 injured. Eighteen buildings were destroyed and 165 buildings were damaged by the earthquake. Focal solution indicated that the Chiayi earthquake is resulted from compressional rupture and displacement along a reverse (backthrust) fault (Wen et al., 2008). Approximately one month before the Chiayi earthquake, the catastrophic Chichi earthquake ($M_L = 7.3$) struck central Taiwan on September 20, 1999. The epicenter of the Chiayi earthquake is located about 55 km south-west of the Chichi earthquake. Using the method of Coulomb failure stress change, Chang and Wang (2006) showed that the static stress changes transferred from the Chichi earthquake may have triggered the Chiayi earthquake.

High quality seismic data of the Chiayi earthquake was recorded from January 1, 1997, to December 31, 2004 via the dense seismic network set up by the Central Weather Bureau (CWB) of Taiwan. Seismicity within Central Taiwan and the study area is shown in Fig. 1. It is clear that the Chiayi earthquake cluster is isolated from the cluster of Chichi earthquake or other clusters. The Chiayi earthquake cluster is centered in the 0.2°×0.3° rectangular zone (longitude: 120.35°E to 120.55°E, latitude: 23.35°N to 23.65°N). As the magnitudes and locations of the low magnitude earthquakes are unreliable, a threshold of the local earthquake magnitude scale of 2 ($M_L \geqq 2$) is used in this study.

Totally 1538 earthquakes of $M_L \geqq 2$ were identified from the record. The temporal distribution of the Chiayi earthquake cluster is shown in Fig. 2(a). Three large earthquakes from August 20 to December 15, 1999, are of interest: the Chichi earthquake, Chiayi earthquake, and the aftershock ($M_L = 5.06$) of the Chiayi earthquake (Fig. 2(b)). As the Chichi earthquake occurred on September 20, 1999, the seismic activity in the Chiayi area became more active since that event. The largest aftershock ($M_L = 6.0$) of the Chiayi earthquake occurred about five hours after the main shock, and the second large aftershock ($M_L = 5.08$)

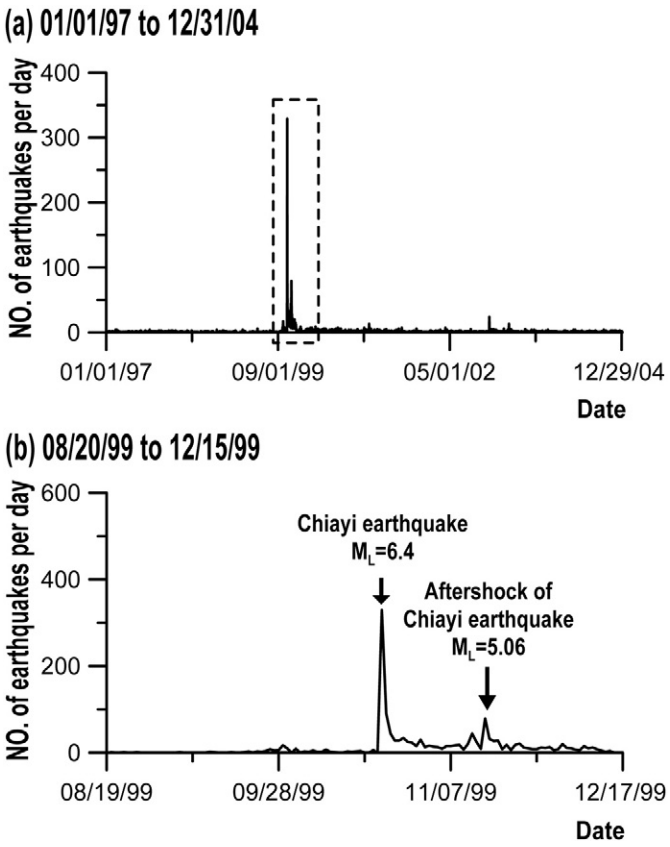

Fig. 2. (a) Temporal distribution of the Chiayi earthquake cluster from January 1, 1997 to December 31, 2004. (b) The interval expanded from the dashed interval in (a). Two large earthquakes are identified during the period from August 20, 1999 to December 15, 1999.

occurred in the next day (October 23, 1999). A large aftershock ($M_L = 5.06$) occurred on November 15, which accompanied a remarkable increase of the number of earthquakes at the same day. The seismic activity in the Chiayi area became stabilized after April 18, 2001. Therefore, four stages of temporal seismicity can be determined for this area. The temporal and spatial distributions of the earthquakes for the four stages are shown in Figs. 3 and 4, respectively. The b values obtained from the Gutenberg–Richter plots for each of the four stages are shown in Fig. 5.

Stage 1 extends from January 1, 1997 to September 20, 1999 and represents the background stage. During this stage, the average number of the earthquakes per day is less than 1 (Fig. 3(a)), and the epicenters distribute randomly (Fig. 4(a)). The b value is almost equal to 1 (b = 0.97), shown in Fig. 5(a). After the Chichi earthquake, the seismicity in the Chiayi area became more active (Fig. 3(b)), and the epicenters of earthquakes in the Chiayi area are getting cluster (Fig. 4(b)). These earthquakes could be considered as the foreshocks before the Chiayi earthquake. This period is referred to as the Stage 2 and extends from September 20 to October 22, 1999. The average number of earthquakes per day in this stage is greater than 1, and the maximum number of earthquakes in a day is 7. The b value is lower (b = 0.83, Fig. 5(b)) than those in the background stages. The Stage 3 extends from October 22, 1999 and ends on April 18, 2001. This stage is determined to be the aftershocks of the Chiayi earthquake. It is seen from Fig. 3(c) that the number of the earthquakes per day varies dramatically. The epicenters get more clustering in space (Fig. 4(c)) and the b (0.81) value is still low (Fig. 5(c)). Seismicity approaches background levels in the Stage 4 from April 18, 2001, to December 31, 2004. The level of seismicity in this stage remains a little higher than that in the Stage 1; however, it is 7.5 times less than the average number of earthquakes occurring during the aftershock sequence (Fig. 3(d)). The distribution of epicenters is random again (Fig. 4(d)) and the b value returns to about 1 (Fig. 5(d)) as same as that in background stage. The number of days, number of earthquakes and the maximum magnitudes of earthquakes within each stage are listed in Table 1.

3. Multifractal spectrum

The temporal and spatial distributions of earthquakes can be considered as fractals with self-similar properties. However, characterizing the complex temporal (or spatial) distributions of earthquakes by using only one fractal dimension may not be comprehensive. The data set with multifractal properties can be considered as an interwoven set with different fractal dimensions (Sprott, 2003). Therefore the multifractal nature of the temporal (or spatial) distributions of earthquakes may implicitly contain several fractal dimensions in the data. The multifractal spectrum is thus a measure of the scaling properties of a data set, which can be characterized by the generalized fractal dimension. The generalized temporal fractal dimension, D_q, can be

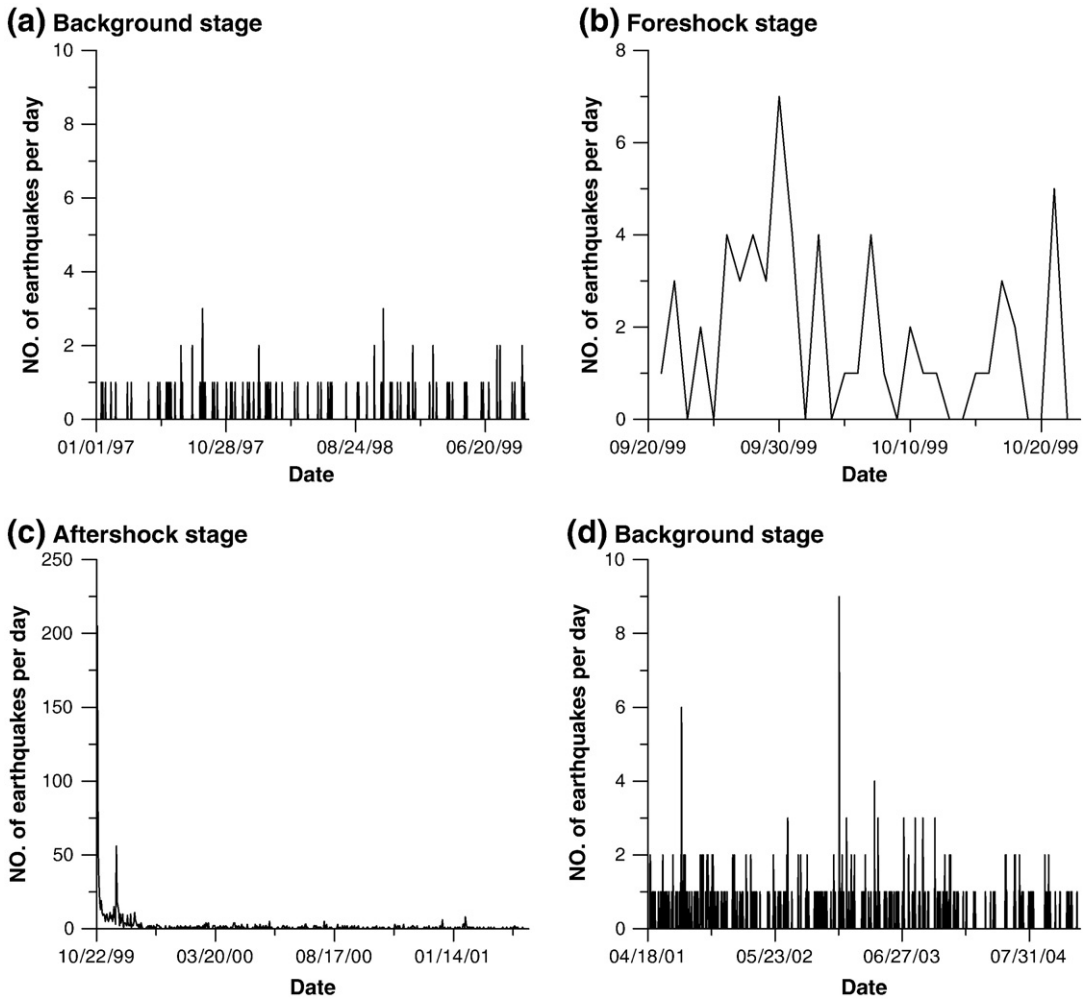

Fig. 3. Number of earthquakes per day in the Chiayi area. (a) The first (background) stage from January 1, 1997, to September 20, 1999. (b) The second (foreshock) stage from September 20 to October 22, 1999. (c) The third (aftershock) stage from October 22, 1999, to April 18, 2001. (d) The fourth (background) stage from April 18, 2001, to December 31, 2004.

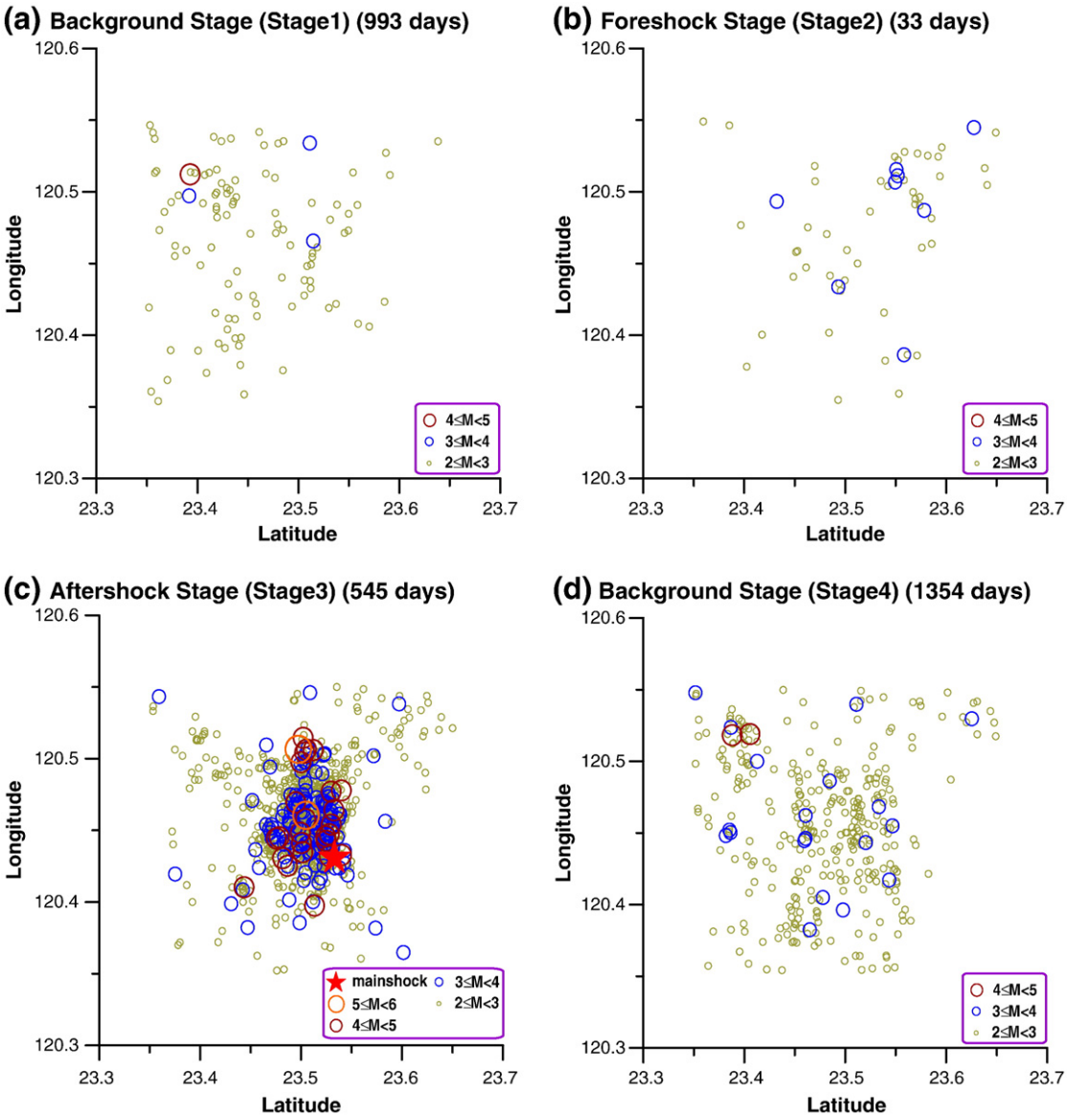

Fig. 4. Spatial distributions of epicenters in the Chiayi area. The red star symbol is the mainshock. (a) The (background) Stage 1. (b) The (foreshock) Stage 2. (c) The (aftershock) Stage 3. (d) The (background) Stage 4.

defined by the following equation (Grassberger and Procaccia, 1983; Hentschel and Procaccia, 1983; Hirata and Imoto, 1991; Kurths and Herzel, 1987):

$$D_q = \lim_{t\to 0} \frac{\log C_q(t)}{\log t} \tag{1}$$

where t is the period between the occurrences of two earthquakes, and $C_q(t)$ is the correlation integral:

$$C_q(t) = \left\{ \frac{1}{N}\sum_{i=1}^{N}\left[\left(\frac{1}{N}\right)\sum_{j=1}^{N}\theta\left(t-\left|T_i-T_j\right|\right)\right]^{q-1} \right\}^{1/(q-1)}, \quad if \begin{cases} t\geq\left|T_i-T_j\right|, & \theta(x)=1 \\ t<\left|T_i-T_j\right|, & \theta(x)=0 \end{cases} \tag{2}$$

where $\theta(x)$ is the Heaviside step function, and N is the number of earthquakes in the study. In Eq. (1), q is the real number in the range $(-\infty, +\infty)$, and T_i and T_j represent the time interval of the i-th and the j-th earthquakes' occurrences, respectively. A linear regression of the $\log(C_q(t))$-$\log(t)$ relationship for each q can be used to estimate the generalized fractal dimension. The generalized fractal dimensions for q = 0, 1 and 2 are named as the capacity dimension (D_0), information dimension (D_1) and correlation dimension (D_2), respectively.

In regressing the D_q values, the upper (t_s) and lower (t_n) boundaries of the scaling interval can avoid the saturation and depopulation of the regression. They can be calculated via the most commonly used correlation dimension (D_2) as (Nerenberg and Essex, 1990):

$$t_s = \frac{t}{D_2+1} \tag{3}$$

$$t_n = 2t\left(\frac{1}{N}\right)^{1/D_2}. \tag{4}$$

Therefore, in each stage we first use all $C_2(t)$ data to estimate a rough D_2 value. Then, substituting this rough D_2 value into Eqs. (3) and (4) can calculate t_s and t_n. Finally, this scaling interval is used to estimate D_q for q = −10 to q = 10. An example of the calculations for the background stage (04/18/2001 ~ 12/31/2004) is shown in Fig. 6.

For positive q values, the D_q represents the fractal dimension of large fluctuations and the value will be low for multifractal time

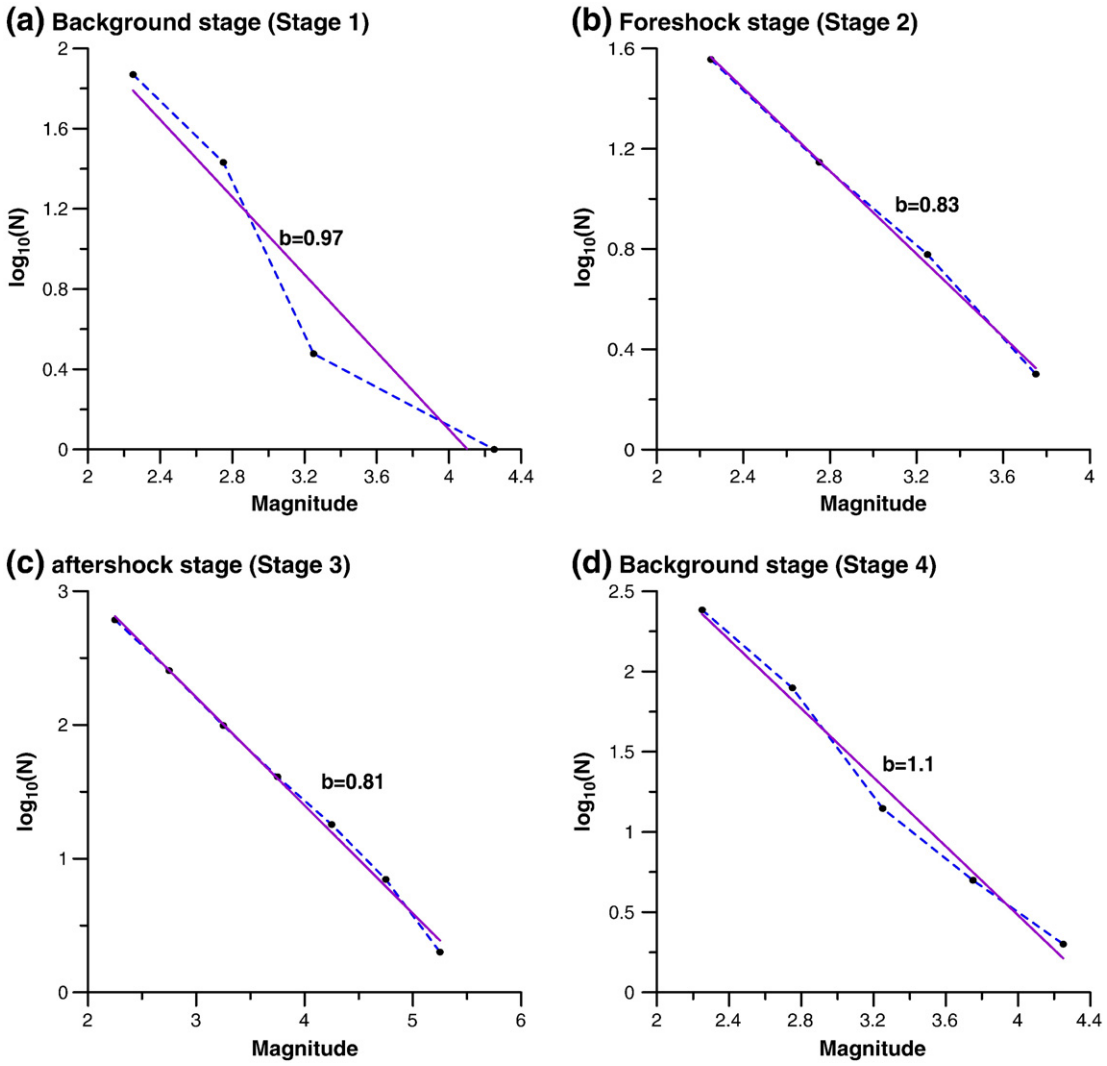

Fig. 5. The b values of the four stages in the Chiayi area with the magnitude threshold of 2.0. (a) Stage 1. (b) Stage 2. (c) Stage 3. (d) Stage 4.

series. But for negative q values, the D_q stands for fractal dimension of small fluctuations and the value will be high for multifractal time series (Sprott, 2003; Telesca et al., 2005). Therefore, in this study, the generalized fractal dimension is helpful for characterizing the temporal seismicities of an earthquake cluster in a small fault area.

4. Results and discussions

To estimate the D_q of the Chiayi earthquake cluster, the q values are selected from −10 to 10 with a step size of 2 for each stage. Estimated D_q values and their 95% confidence intervals for each stage are shown in Fig. 7. The degree of the multifractality can be represented by the difference between D_{-10} and D_{10} and is referred to as the multifractal degree (Telesca et al., 2005). Hence, we interpret the Stage 1 as the background seismicity because its D_q curve is fairly smooth and its multifractal degree is about 0.36. The small 95% confidence intervals indicate that the D_q values of the Stage 1 are reliable. However, the D_q curve for Stage 2 (the period of enhanced seismicity rate prior to the mainshock) begins to deviate from the Stage 1 response. Instead of gradually dropping as in Stage 1 it retains nearly constant D_q out to $q = -2$. From there, it drops more steeply between $q = -2$ and $q = 4$. For q higher than 4, Stages 1 and 2 responses coincide. Multifractal degree during Stage 2 remains almost the same as that of Stage 1. Deviation from the Stage 1 response and the steep slope at D_0 are characteristics of Stage 2. In this stage, the 95% confidences are much larger due to the scarcity of data. However, the deviations observed between $q = -2$ and $q = 0$ are significant. When the Stage 2 transfers to Stage 3 (aftershock), the D_q values drop dramatically from 1.18 at $q = -10$ to 0.24 at $q = 10$, and the multifractal degree increases to 1.0. Nevertheless, the small 95% confidence interval indicates that the results are reliable. Stage 4 marks a return to background seismicity. D_q

Table 1
Numbers of days, earthquakes and maximum magnitude in the four stages of the Chiayi earthquake.

	Background stage (Stage 1)	Foreshock stage (Stage 2)	Aftershock stage (Stage 3)	Background stage (Stage 4)
Period	01/01/97 ~ 09/20/99	09/20/99 ~ 10/22/99	10/22/99 ~ 04/18/01	04/18/01 ~ 12/31/04
Days	993	33	545	1354
No. of earthquakes	105	58	1033	342
Maximum magnitude	4.0	3.7	6.4	4.5

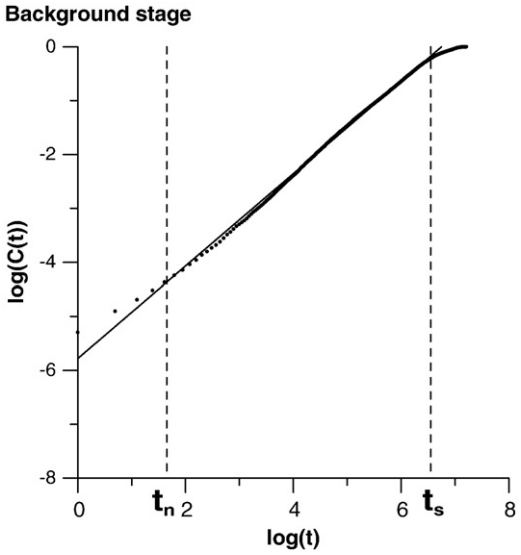

Fig. 6. Plot of the correlation function versus correlation time for q = 2. t_n and t_s are the lower and upper boundaries of the correlation time t.

remains slightly higher but closely parallels the Stage 1 response. The multifractal degree is the same as that of Stage 1 (0.36). The small confidence interval of this stage indicates that the estimated D_q values are of the same accuracy as those of the Stage 1. In summary, distinct differences in multifractal behavior are observed in the foreshock and aftershock events associated with the Chiayi earthquake.

In order to test whether the number and threshold magnitude of earthquakes can affect the calculation of the temporal multifractal dimension of the Chiayi earthquake cluster, two tests were performed. In the first test, six test data sets were made and each test data set contains 100 earthquakes which were randomly selected from those of the Stage 3. The threshold magnitudes of earthquakes are $M_L \geqq 0$ for three test data sets and $M_L \geqq 2$ for the other three. The earthquakes in the test data sets are shown in Fig. 8 and their D_q curves are shown in Fig. 9. For $q \leqq 0$, the D_q values indicate the local dimension in the most sparsely populated region (Sprott, 2003) and degree of the small fluctuation of the population (Telesca et al., 2005). For both $M_L \geqq 0$ and $M_L \geqq 2$, the D_q curves are steady or descending with the q value when $q \leqq 0$. That represents not only the low density of the number of earthquakes in all test data sets but also the homogeneous distribution of

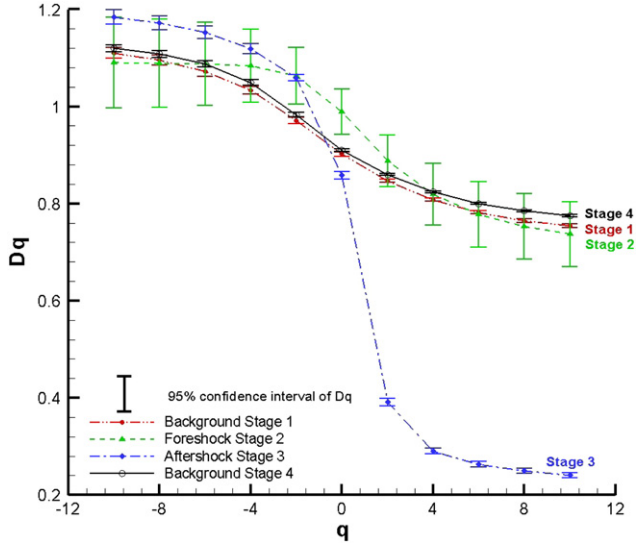

Fig. 7. Fluctuations of the generalized fractal dimensions D_q (q = −10 to q = 10) and their 95% confidence intervals for the four stages of the Chiayi earthquake.

earthquakes within the chosen period. On the contrary, all D_q curves of test data sets are similar to the original one when $q \geqq 0$ despite that the earthquake numbers of test data sets are significantly smaller than that in the Stage 3. For the second test, the D_q values in the foreshock stage are calculated for earthquakes with magnitudes $M_L \geqq 0$ and $M_L \geqq 2$ (Fig. 10), and the numbers of earthquakes in the data sets are 110 and 58, respectively. Fig. 10 shows that their multifractal properties are alike. Therefore, based on the two tests we can conclude that the number and threshold magnitude of earthquakes do not influence the calculation of the multifractal property significantly.

The large fluctuation of D_q of the spatial distribution of earthquakes in the range $D_2 \sim D_\infty$ generally means an increase in the heterogeneity of the earthquakes distributions (Lei et al., 1993). The same idea can be used to the D_q of the temporal distribution of earthquakes. In the Stage 1, the D_q curve is smooth with negligible fluctuation. Therefore, the earthquake cluster in the background stage is considered to be nearly homogeneous (or nearly monofractal) in the temporal distribution of earthquakes. Nearly monofractal dimension means that the fractal dimension is insensitive with q. For the Stage 2, the earthquake cluster has evolved to be heterogeneous and multifractal as the D_q curve is more fluctuant than that in the background stage. Following the same line, the earthquake cluster in the Stage 3 should be the most heterogeneous and strongly multifractal with the largest multifractal degree because the fluctuation of the D_q in this stage is the largest. Finally, characteristics of the earthquake cluster in the Stage 4 should be similar to that in the Stage 1 because both of which show approximately the same pattern of the D_q curve and the same multifractal degree. Therefore the temporal multifractal property of seismicity becomes noticeable when the seismicity becomes active, and vice versa.

In addition, we used the moving window method to calculate the D_q curves of the Chiayi earthquakes with $M \geqq 2$ (Fig. 11). The window length is 33 days except the window A which is from Jan. 1, 1997 to Sep. 20, 1999 because of too few earthquakes at background stage within 33 days window length to calculate the D_q curve. The D_q curve of the window A is smooth. When the window is moved to B position which straddles the background and foreshock stages, the D_q curve becomes more curvy than those of window A especially with a significant slope change around the q = 0. For the window C which is within the foreshock stage, the D_q curve returns and is similar to those of window A. Therefore using the moving window to scan the temporal relationships of earthquakes of an area, the change of slope of D_q curve at q = 0 may be used as an indicator for the foreshock. A similar variation is observed from windows C to E but more violent. Window D straddles the foreshock and aftershock stages, the D_q curve is curviest and the fractal degree is largest among all windows. Window E is within the aftershock stage, the fractal degree is smaller than that of window D but it is still larger than others. From windows F to G, their D_q curves are becoming smooth gradually.

According to the results of the moving window analysis, if the window straddles two different stages (two different populations of data), the D_q values will vary significantly since this method enhances the contrast between the short and long temporal correlations of earthquakes. As a result, a large fluctuation of D_q is produced. This will lead to a misinterpretation that the study area is under a strong heterogeneous state. For our study area, however, each stage has its own seismogenic characteristic and seismicity. Therefore, multifractal characteristics of a stage can only be revealed by that stage's seismic data. According to Rossi (1990), the fractal dimension in the spatial distributions of hypocenters (D_F) decreases before and after a large earthquake. Nevertheless, our results (Figs. 7 and 11) show that D_q for $q \geq 2$ also decreases before and even after a large earthquake but the D_q increases for $q \leq -2$. Additionally, D_q values for q = 0 are almost the same in all stages. This means that D_0 is relatively insensitive to the seismicity in time. This result is consistent with the conclusion of Wang and Lee (1996) that D_0 is not able to distinguish spatial fractal properties of earthquakes.

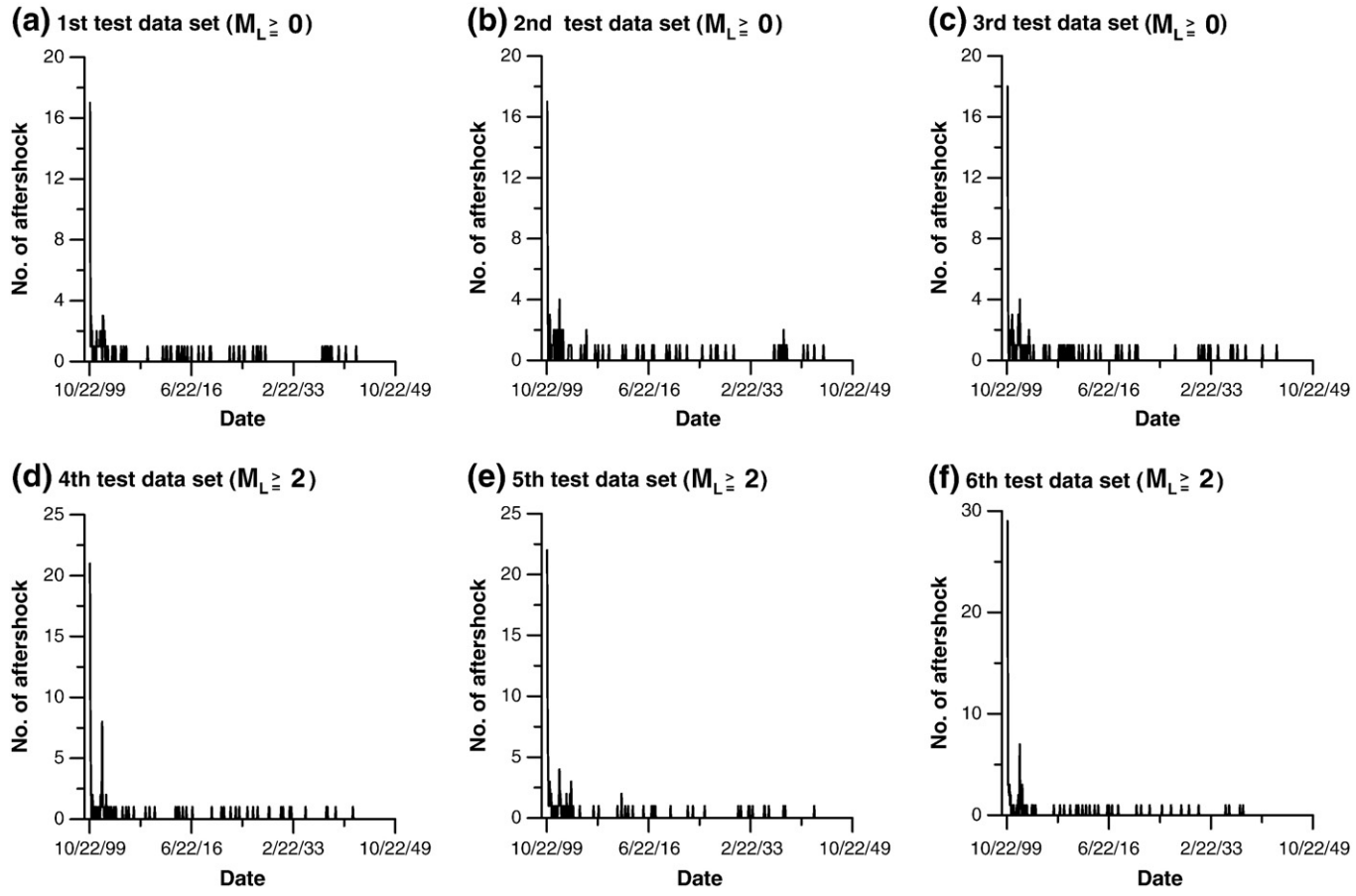

Fig. 8. Earthquake sequences of six test data sets and each containing 100 earthquakes which were randomly selected from the aftershock stage with $M_L \geq 0$ (a) to (c) and $M_L \geq 2$ (d) to (f).

Below we summarize the temporal multifractal properties of the four stages identified in retrospect from the Chiayi earthquake:

Background Stage (Stage 1): The fluctuation of D_q from $q = -10$ to 10 for the background seismicity in the Chiayi area is smaller than those of other stages with the multifractal degree of D_q being less than 0.36. The average value of D_q in this stage is about 1. This nearly monofractal property may mean that the background seismicity is generated by a stochastic process (Godano and Caruso, 1995; Godano et al., 1999). Hence the background seismicity of the Chiayi earthquake can be regarded as a result of nearly monofractal stochastic process.

Foreshock Stage (Stage 2): The seismicity during the foreshock stage increases in frequency. D_q drops more steeply from negative to positive q (Fig. 7). In the foreshock

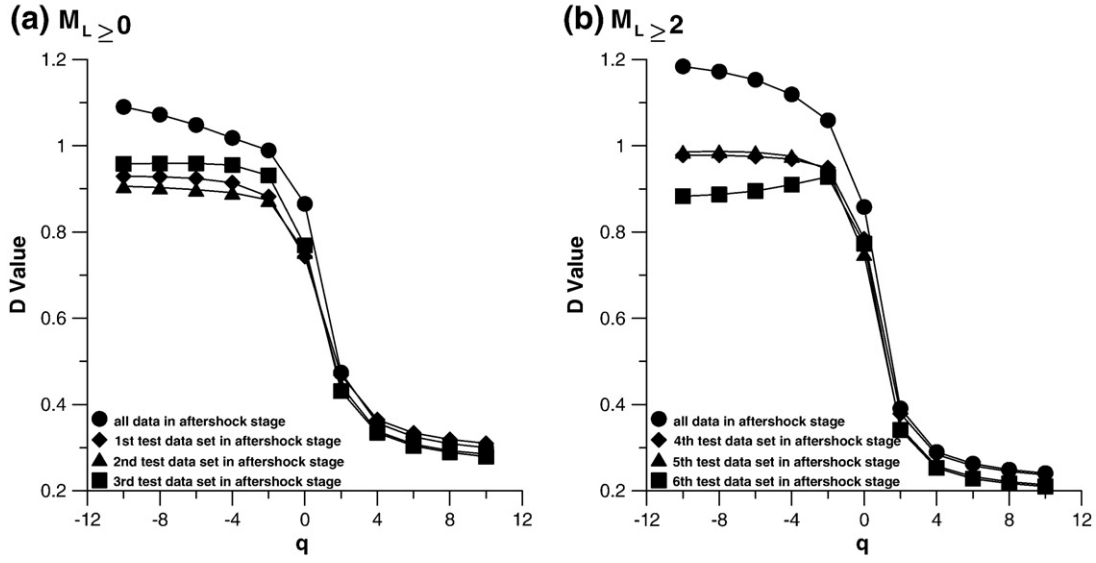

Fig. 9. The D values of six test data sets and each containing 100 earthquakes which were randomly selected from the aftershock stage with (a) $M_L \geq 0$ and (b) $M_L \geq 2$.

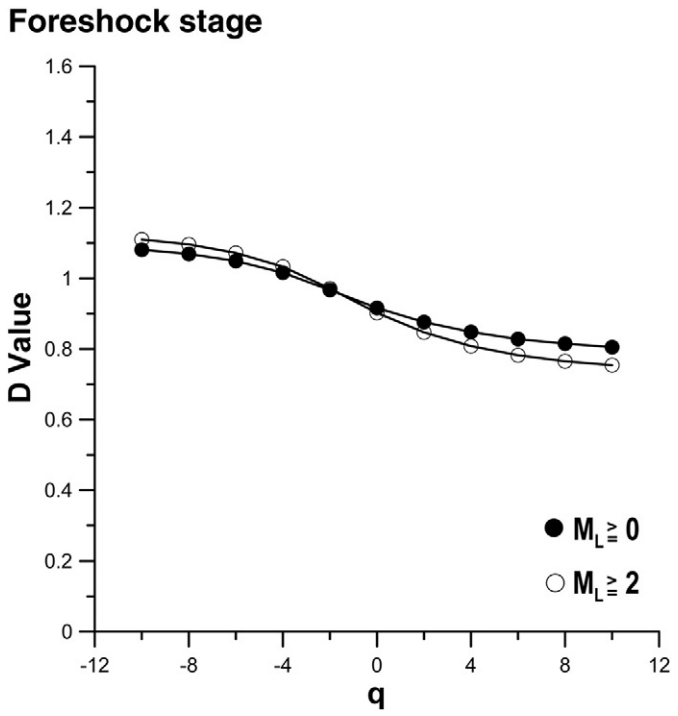

Fig. 10. The D values of the foreshock stage with different threshold magnitude ($M_L \geq 0$ and $M_L \geq 2$).

stage, the spatial fractal dimension decreases with time because of the active seismicity before a large earthquake (Godano et al., 1999; Kiyashchenko et al., 2003; Nakaya and Hashimoto, 2002). However for the Chiayi earthquakes, the D_q is higher than the background Stage 1 data roughly between q equal −2 to 0. In addition, a drop in b value is also observed in this stage which is consistent with the conclusions of Suyehiro (1966), Henderson et al. (1992) and Smith (1998). It is known that the variation of the multifractal properties of earthquakes is caused by the changes in the seismogenic regime (Mittag, 2003). Furthermore, the static stress changes in the Chiayi area, which is simulated by the observed creep rate variations with regard to the velocity-strengthening friction law and 1-D groundwater diffusion model, were transferred from the Chichi earthquake (Chang and Wang, 2006). In addition, the anomalous diurnal variations of geomagnetic field and resistivity before the Chiayi earthquake were observed (Liu et al., 2001, 2006; Tsai et al., 2006; Yen et al., 2004). The foreshock period is characterized not only by anomalous seismic behavior, but is accompanied by anomalous geomagnetic and electrical behaviors as well.

Aftershock Stage (Stage 3): In the aftershock stage, D_0 is close to 0.86 but D_{10} drops to 0.24, the lowest value of D_q. The difference between D_0 and D_{10} of this stage is the greatest in all of the four stages, and the multifractal degree is also the largest one (1.0). Therefore, the temporal multifractal property of the aftershock stage is clearly observed, and the heterogeneity of the seismicity in the aftershock stage is the strongest in all of the four stages.

Aftershock is a procedure of releasing energy (Utsu, 1961). The released energy reduces with time, and the numbers of the aftershocks also decrease over time (Omori, 1894). Furthermore, there are two diffusive aftershock mechanisms (Telesca et al., 2005): 1) Mainshock does not release the stress completely. 2) The stress field is modified after mainshock. These theories imply that energy accumulation and energy release processes co-exist in aftershocks. Therefore, the seismogenic mechanics in the aftershock stage is under a stress-adjusting state. Accordingly, the seismogenic regime in the Chiayi area becomes more complex and active. This complex seismogenic system yields the significant temporal aftershock distributions and the complex temporal multifractal properties.

Background Stage (Stage 4): After the aftershock stage, the seismicity in the Chiayi region returns to the background seismicity

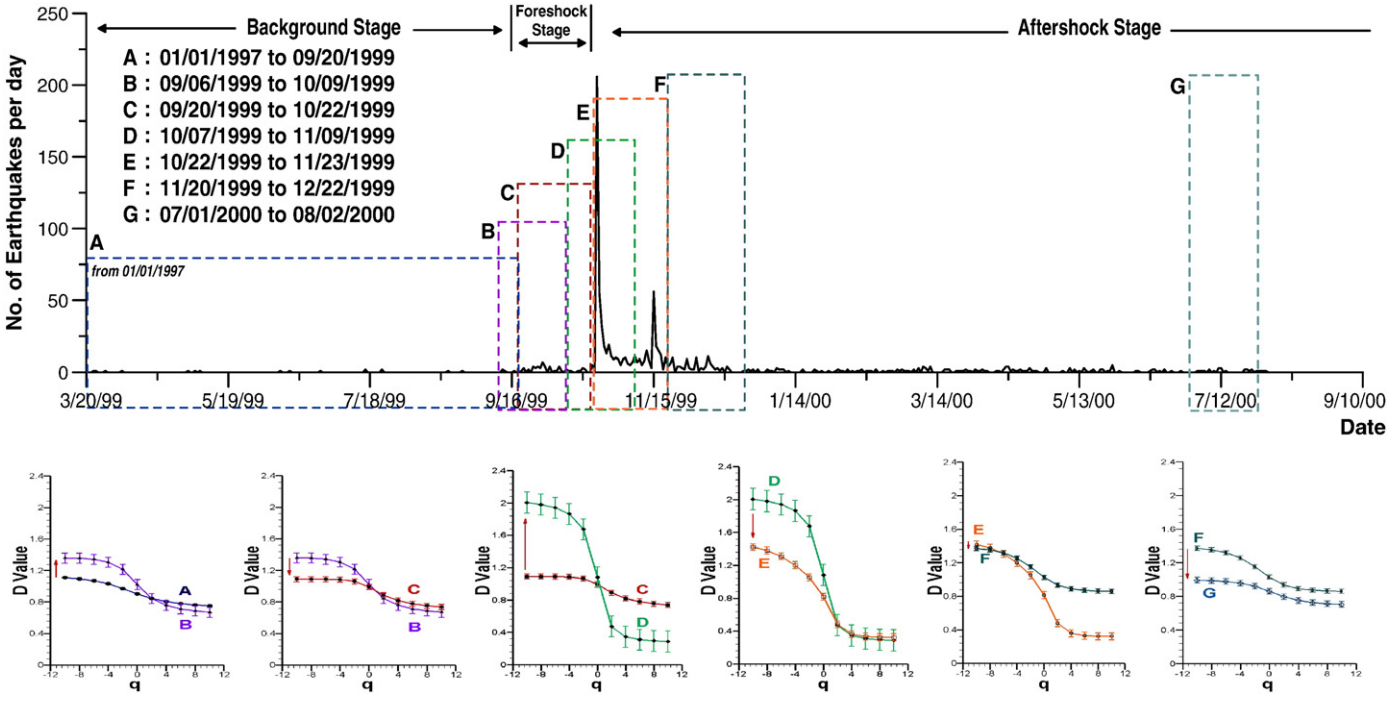

Fig. 11. The D_q values of the seismicities within the windows are calculated at 7 different time positions (A–G) from the background, foreshock stages and to the aftershock stage.

with the same multifractal degree as that in the Stage 1. Therefore, the temporal multifractal spectrum of seismicity in the aftershock stage becomes more stabile.

5. Conclusions

The fluctuations in the temporal multifractal dimension of the Chiayi earthquake cluster reveal significant differences between temporal seismogenic regimes. For the background seismicity, the D_q drops sinusoidally from about 1.12 to 0.8 as q increases from −10 to 10. A distinct foreshock stage is observed in the multifractal curve (Stage 2). It deviates from the background response and remains higher for q between −4 and 4. These differences are statistically significant between q of −2 and 2. In the aftershock stage (Stage 3), D_q drops from about 1.1 to .4 as q increases from −2 to 2 which is much larger than those in the other stages. Over the entire range, D_q has multifractal degree of about 1 (dropping from about 1.2 to 0.24). Finally, the seismicity returns to background levels (Stage 4) and the D_q curve takes on the smoother sinusoidal variations characteristic of Stage 1.

This study illustrates that the variations in the temporal generalized fractal dimension of an earthquake sequence can reveal statistically significant differences between the various stages associated with background, foreshock and aftershock seismic behavior. The statistically significant changes of D_q curve are observed in the slope at D_0 and suggest these measures may be used to identify precursor activity.

References

Aviles, C.A., Scholz, C.H., Boatwright, J., 1987. Fractal analysis applied to characteristic segments of the San Andreas fault. Journal of Geophysical Research 92, 331–344.

Chang, S.H., Wang, W.H., 2006. Mechanical properties, slip and nucleation of the 1999 Chiayi earthquake. TAO 17, 331–343.

Chang, Y.F., Chen, C.C., Liang, C.Y., 2007. The fractal geometry of the surface ruptures of the 1999 Chi-Chi earthquake, Taiwan. Geophysical Journal International 170, 170–174.

Godano, C., Caruso, V., 1995. Multifractal analysis of earthquake catalogues. Geophysical Journal International 121, 385–392.

Godano, C., Tosi, P., Derubeis, V., Augliera, P., 1999. Scaling properties of the spatio-temporal distribution of earthquakes: a multifractal approach applied to a California catalogue. Geophysical Journal International 136, 99–108.

Grassberger, P., Procaccia, I., 1983. Measuring the strangeness of strange attractors. Physica 9D, 189–208.

Guo, Z., Ogata, Y., 1995. Correlation between characteristic parameters of aftershock distributions in time, space and magnitude. Geophysical Research Letters 22, 993–996.

Henderson, J., Main, I., Meredith, P., Sammonds, P., 1992. The evolution of seismicity at Parkfield: observation, experiment and a fracture-mechanical interpretation. Journal of Structural Geology 14, 905–913.

Henderson, J.R., Barton, D.J., Foulger, G.R., 1999. Fractal clustering of induced seismicity in the Geysers geothermal area, California. Geophysical Journal International 139, 317–324.

Hentschel, H.G.E., Procaccia, I., 1983. The infinite number of generalized dimensions of fractals and strange attractors. Physica 8D, 435–444.

Hirabayashi, T., Ito, K., Yoshii, T., 1992. Multifractal analysis of earthquakes. PAGEOPH 138, 591–610.

Hirata, T., Imoto, M., 1991. Multifractal analysis of spatial distribution of microearthquakes in the Kanto region. Geophysical Journal International 107, 155–162.

Kiyashchenko, D., Smirnova, N., Troyan, V., Vallianatos, F., 2003. Dynamics of multifractal and correlation characteristics of the spatio-temporal distribution of regional seismicity before the strong earthquakes. Natural Hazards and Earth System Sciences 3, 285–298.

Kurths, J., Herzel, H., 1987. An attractor in a solar time series. Physica 25D, 165–172.

Lei, X., Nishizawa, O., Kusunose, K., 1993. Band-limited heterogeneous fractal structure of earthquakes and acoustic-emission events. Geophysical Journal International 115, 79–84.

Liu, J.Y., Chen, Y.I., Chuo, Y.J., Tsai, H.F., 2001. Variations of ionospheric total electron content during the Chi-Chi earthquake. Geophysical Research Letters 28, 1383–1386.

Liu, J.Y., Chen, C.H., Chen, Y.I., Yen, H.Y., Hattori, K., Yumoto, K., 2006. Seismogenic geomagnetic anomalies and M≧5.0 earthquakes observed in Taiwan during 1988–2001. Physics and Chemistry of the Earth 31, 215–222.

Mandelbrot, B.B., 1967. How long is the coast of Britain? Statistical self-similarity and fractional dimension. Science 156, 636–638.

Mandelbrot, B.B., 1989. Multifractal measures, especially for the geophysicist. PAGEOPH 131, 5–42.

Mittag, R.J., 2003. Fractal analysis of earthquake swarms of Vogtland/NW-Bohemia intraplate seismicity. Journal of Geodynamics 35, 173–189.

Nakaya, S., Hashimoto, T., 2002. Temporal variation of multifractal properties of seismicity in the region affected by the main shock of the October 6, 2000 western Tottori Prefecture, Japan, earthquake (M = 7.3). Geophysical Research Letters 29 (art. no.-1495).

Nerenberg, M.A.H., Essex, C., 1990. Correlation dimension and systematic geometric effects. Physical Review A 42, 7065–7074.

Okubo, P.G., Aki, K., 1987. Fractal geometry in the San Andreas fault system. Journal of Geophysical Research 92, 345–355.

Omori, F., 1894. On after-shocks of earthquakes. The Journal of the College of Science, Imperial University of Tokyo 7, 111–200.

Öncel, A.O., Main, I., Alptekin, Ö., Cowie, P., 1996. Spatial variations of the fractal properties of seismicity in the Anatolian fault zones. Tectonophysics 257, 189–202.

Papadopoulos, G.A., Dedousis, V., 1992. Fractal approach of the temporal distribution in the Hellenic arc-trench system. PAGEOPH 139, 269–276.

Rossi, G., 1990. Fractal dimension time variations in the Friulu (Northeastern Italy) seismic area. Bollettino di Geofisica Teorica ed Applicata 32, 175–184.

Smith, W.D., 1998. Resolution and significance assessment of precursory changes in mean earthquake magnitudes. Geophysical Journal International 135, 515–522.

Sprott, J.C., 2003. Chaos and time-series analysis. Oxford Univ. Press, Oxford.

Sukmono, S., 2001. New evidence on the fractal pattern of Sumatra fault seismicity and its possible application to earthquake prediction. Bulletin of the Seismological Society of America 91, 870–874.

Suyehiro, S., 1966. Difference between aftershocks and foreshocks in the relationship of magnitude to frequency of occurrence for the great Chilean earthquake of 1960. Bulletin of the Seismological Society of America 56, 185–200.

Telesca, L., Lapenna, V., Macchiato, M., 2005. Multifractal fluctuations in seismic interspike series. Physica A 354, 629–640.

Tsai, Y.B., Liu, J.Y., Ma, K.F., Yen, H.Y., Chen, K.S., Chen, Y.I., Lee, C.P., 2006. Precursory phenomena associated with the 1999 Chi-Chi earthquake in Taiwan as identified under the iSTEP program. Physics and Chemistry of the Earth 31, 365–377.

Utsu, T., 1961. A statistical study on the occurrence of aftershocks. Geophysical Magazine 30, 521–605.

Wang, J.H., Lee, C.W., 1996. Multifractal measures of earthquakes in west Taiwan. PAGEOPH 146, 131–145.

Wen, S., Chen, C.H., Teng, T.L., 2008. Ruptures in a highly fractured upper crust. PAGEOPH 165, 201–213.

Yen, H.Y., Chen, C.H., Yeh, Y.H., Liu, J.Y., Lin, C.R., Tsai, Y.B., 2004. Geomagnetic fluctuations during the 1999 Chi-Chi earthquake in Taiwan. Earth Planets Space 56, 39–45.